Shear Wavelength Estimation Based on Inverse Filtering and Multiple-point Shear Wave Generation

多点励振と逆フィルタによる剪断波の波長推定

Tomoaki Kitazaki1[‡], Kengo Kondo, Makoto Yamakawa and Tsuyoshi Shiina (Graduate School of Medicine, Kyoto Univ.)

北﨑智明[‡], 近藤健悟, 山川誠, 椎名毅 (京都大院 医)

1. Introduction

Elastography provides important diagnostic information regarding tissue stiffness. For example, in a mammary grand, higher grade malignancies yield harder tumors [1]. Estimating shear wave speed enables the quantification of tissue elasticity imaging. Acoustic radiation force (ARF) has been used to produce shear waves, and the time-of-flight is measured to determine the shear wave speed [2]. However, the method is based on an assumption about the propagating direction of a shear wave that is highly affected by reflection and refraction and thus might cause an artifact.

To overcome this limitation, we proposed a new method for shear wave elasticity imaging which combines a shear wavelength approach and inverse filtering with the multiple shear wave sources induced by ARF [3]. Shear wave generation can be controlled by using ARF sources. An inverse filter can focus a point in a reverberant field. Thus, the proposed method is not based on the assumption of the propagating direction, and improved estimation accuracy can be expected.

In this study, we propose an alternative approach to measure a shear wavelength and demonstrate its feasibility with a phantom experiment.

2. Methods of Elasticity Imaging

2. 1. Overall flow

Shear waves are induced by ARF, recorded by ultrafast imaging, and repeated at multiple pushing points which are sparsely located. Assuming that shear waves obtained by each shear wave source is approximated as impulse responses, an inverse filter [4] can be applied to virtually focus a shear wave on an arbitrary point. Measuring the full width at half maximum of the focal point is equivalent to the half-wavelength of the shear wave [5]. Thus, it is approximated as the half-wavelength that measuring the distance across through the cross-sectional area of the focal point at half maximum.

The shear wave speed can be measured by calculating the product of the shear wavelength and the frequency. The shear-elasticity is obtained through the shear wave speed. By scanning the focal point, the shear-elasticity image can be obtained.

2.2 Inverse filter

In the Fourier domain, receiving column vector $\mathbf{R}(\omega)$ is given by

$$\mathbf{R}(\omega) = \mathbf{H}(\omega) \cdot \mathbf{E}(\omega), \qquad (1)$$

Here, ω is the given angular frequency, $\mathbf{H}(\omega)$ is the propagation matrix, $\mathbf{E}(\omega)$ is the emission column vector. To focus shear waves on j, an objective vector $\mathbf{R}_j^{IF}(\omega)$ can be writtern as $\mathbf{R}_j^{IF}(\omega) = (0,...,1,...,0)$. $\mathbf{R}_j^{IF}(\omega)$ is given by

$$\mathbf{R}_j^{IF}(\omega) = \mathbf{H}(\omega) \cdot \mathbf{E}_j^{IF}(\omega). \qquad (2)$$

$\mathbf{R}_j^{IF}(\omega)$ and $\mathbf{H}(\omega)$ are given. To find $\mathbf{E}_j^{IF}(\omega)$, calculate the inverse matrix $\mathbf{H}^{-1}(\omega)$. However, this process magnifies errors by inversion of noise componets. To avoid such a problem, a singular value decomposition of $\mathbf{H}(\omega)$ is performed before inversion. The matrix inversion is only applied to the main singular vectors of the singular value decomposition of $\mathbf{H}(\omega)$. The ideal emission $\widetilde{\mathbf{E}}_j^{IF}(\omega)$ is then derived by

$$\widetilde{\mathbf{H}}^{-1}(\omega) \cdot \mathbf{R}_j^{IF}(\omega) = \widetilde{\mathbf{H}}^{-1}(\omega) \cdot \mathbf{H}(\omega) \cdot \mathbf{E}_j^{IF}(\omega)$$
$$= \widetilde{\mathbf{E}}_j^{IF}(\omega), \qquad (3)$$

where $\widetilde{\mathbf{H}}^{-1}(\omega)$ is the noise-filtered inverse matrix. The optimal focusing $\boldsymbol{\psi}_j(\omega)$ will be given by

$$\boldsymbol{\psi}_j(\omega) = \mathbf{H}(\omega) \cdot \widetilde{\mathbf{H}}^{-1}(\omega) \cdot \mathbf{R}_j^{IF}(\omega). \qquad (4)$$

Figure 1 shows a simulation of 2D map of the focused shear waves on a point in the ROI by an inverse filter with a single frequency. The black circle of the focused shear wave is a half maximum contour line to measure shear wavelength. The distance across of the circle is equivalent to the half-wavelength.
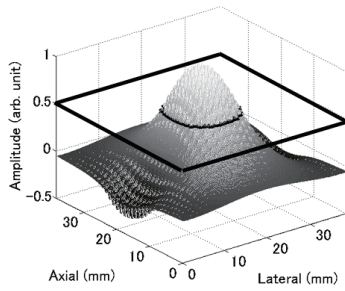
Fig. 1 2D map of the focused shear wave in a simulation.

3. Experimental Condition

An ultrasound system with a 128-channel linear-array transducer (Verasonics, USA) was used to implement the proposed method. The center frequency is 5 MHz, and the frame rate is 5 kHz. Multiple pushing points were sparsely generated.

This experiment was conducted in an elasticity phantom with 10 mm diameter hard inclusions (OST, Japan). The characteristics given by the manufacturer are 40, 60, 80, and 100 kPa for the inclusions and 10 kPa for the background (BG). In this study, we measured the inclusion of 60 kPa. **Figure 2(a)** shows a schematic view of the experiment conditions. **Figure 2(b)** depicts the B-mode that indicates the border of a hard inclusion and BG.

4. Experimental validation

Figure 3(a) shows the estimated elasticity image of nearby the hard inclusion. **Figure 3(b)** shows the profile along the dotted line in Fig. 3(a).

The proposed method can visualize the hard inclusion. The inclusion border depicted in the profile accords closely with the border in B-mode. However, there is X-shaped artifact around the inclusion in Fig. 3(a). One of the reasons is pushing condition. The proposed method needs enough impulse responses, thus pushing condition has great effect on an elasticity imaging.

The feasibility of the proposed method was verified, but we have to improve estimation accuracy nearby an inclusion.
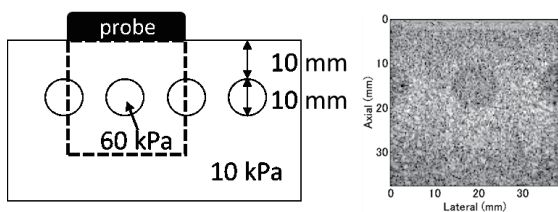
Fig. 2(a) Schematic view of experimental condition. (b) B-mode of the elasticity phantom.
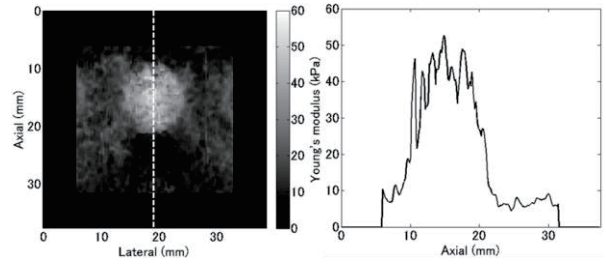
Fig. 3(a) Estimated elasticity image and (b) axial profile of the proposed method.

5. Conclusions

We proposed a new method to measure a shear wavelength. The feasibility of the proposed method was verified using an elasticity phantom. The estimated elasticity image clearly revealed the hard inclusion.

Future works need to improve estimation accuracy nearby an inclusion and confirm usefulness of the proposed method by comparison with the conventional method.

References
1. A. Samani, J. Zubovits, and D. Plewes: Phys. Med. Biol. 52, (2007) 1565.
2. M. Tanter, J. Bercoff, A. Athanasiou, T. Deffieux, J. L. Gennisson, G. Montaldo, M. Muller, A. Tardivon, and M. Fink: Ultrasound in Med. & Biol., Vol. 34, No. 9, (2008) 1373.
3. T. Kitazaki, K. Kondo, M. Yamakawa, and T. Shiina: Proc. of IEEE Int. Ultrason. Sym. (2014) 1121.
4. M. Tanter, J. F. Aubry, J. Gerber, J. L. Thomas, and M. Fink: J. Acoust. Soc. Am., vol. 110, (2001) 37.
5. N. Benech, S. Catheline, J. Brum, T. Gallot, and C. A. Negreria: IEEE Trans. Ultrason. Ferroelctr. Freq. Control, vol. 56, (2009) 2400.